

See discussions, stats, and author profiles for this publication at: <https://www.researchgate.net/publication/231732848>

Synthesis, Structures, Photoluminescent Behaviors, and DFT Studies of Novel Aluminum Complexes Containing Phenoxybenzotriazole Derivatives

ARTICLE *in* ORGANOMETALLICS · DECEMBER 2009

Impact Factor: 4.13 · DOI: 10.1021/om9007423

CITATIONS

13

READS

28

10 AUTHORS, INCLUDING:



Junseong Lee

Chonnam National University

97 PUBLICATIONS 986 CITATIONS

SEE PROFILE



Yoon Sup Lee

Korea Advanced Institute of Science and Tec...

211 PUBLICATIONS 4,407 CITATIONS

SEE PROFILE

Synthesis, Structures, Photoluminescent Behaviors, and DFT Studies of Novel Aluminum Complexes Containing Phenoxybenzotriazole Derivatives

Junseong Lee,[†] So Han Kim,[‡] Kang Mun Lee,[†] Kyu Young Hwang,[†] Hyoseok Kim,[†] Jung Oh Huh,[†] Da Jung Kim,[‡] Yoon Sup Lee,[†] Youngkyu Do,^{*,†} and Youngjo Kim^{*,†}[†]Department of Chemistry, KAIST, Daejeon 305-701, Korea and[‡]Department of Chemistry, Chungbuk National University, Cheongju, Chungbuk 361-763, Korea

Received August 26, 2009

Treatment of AlMe_3 with 2 equiv of 2-(2*H*-benzo[*d*][1,2,3]triazol-2-yl)-4,6-di-*tert*-pentylphenol (**Lig¹H**) or 2-*tert*-butyl-6-(5-chloro-2*H*-benzo[*d*][1,2,3] triazol-2-yl)-4-methylphenol (**Lig²H**) and subsequent addition of ROH afford monomeric and heteroleptic (OR) AlL_2 complexes [**R** = C_6H_5 , **L** = **Lig¹**, **1**; **R** = *p*- $\text{C}_6\text{H}_4\text{Ph}$, **L** = **Lig¹**, **2**; **R** = C_6H_5 , **L** = **Lig²**, **3**; **R** = *p*- $\text{C}_6\text{H}_4\text{Ph}$, **L** = **Lig²**, **4**]. The simple reaction between a quantitative amount of water and compound **1** gave the novel dimeric aluminum complex **5** bridged by an oxygen atom. The crystal structures of **1**, **3**, and **5** determined from X-ray diffraction studies reveal pentacoordination geometry around the Al center with the preference for the slightly distorted trigonal-bipyramidal geometry. Monomeric complexes **1–4** showed emissions of the blue region (475 nm) with broad emission areas (half-width of peak = 150 nm) in the emission spectrum with high quantum yield. Dimeric aluminum complex **5** with enhanced thermal stability has a similar absorption and emission pattern to complexes **1** and **2**, as predicted by DFT calculations. The DFT calculations suggested that the HOMO and LUMO orbitals are localized on the phenoxy group and benzotriazole group of the ligand and the effect of the phenoxide ligand is negligible.

Introduction

The development of new, efficient emitting systems has been of scientific interest and a technologically important subject since the discovery of OLED (organic light-emitting diodes) materials.¹ For full-color displays, red-, green-, and blue-emitting materials are essential. Nevertheless, the known blue-light-emitting materials are far from satisfactory, particularly compared with green and red materials.²

Tris(8-hydroxyquinolino)aluminum (AlQ_3), which has three five-membered rings and shows a green-emitting property (520 nm), is well known among emitting material systems.³ The introduction of electronic effects in the 2,4-

or 5,7-position of ligand Q in AlQ_3 could cause a red or blue shift, as has been well documented in the literature, although reported modified AlQ_3 species showed some thermal instability.^{2a,4} While most previous work has focused on color tuning via the introduction of an electronic effect to homoleptic aluminum complexes with three five-membered chelating rings⁵ or the synthesis of heteroleptic aluminum complexes with one or two five-membered chelating rings,⁶ much less attention has been directed toward the synthesis of homoleptic or heteroleptic aluminum complexes with six-membered chelating rings.⁷ Moreover, there is no

*To whom correspondence should be addressed. e-mail: ykim@chungbuk.ac.kr (Y.K.) or ykdo@kaist.ac.kr (Y.D.). Tel: +82-43-261-3395. Fax: +82-43-267-2279.

(1) (a) Tang, C. W.; VanSlyke, S. A. *Appl. Phys. Lett.* **1989**, *51*, 913. (b) Tang, C. W.; VanSlyke, S. A. *J. Appl. Phys.* **1989**, *65*, 3610.

(2) (a) Perez-Bolivar, C.; Montes, V. A.; Anzenbacher, P., Jr. *Inorg. Chem.* **2006**, *45*, 9610. (b) Kafafi, Z. H., *Organic Electroluminescence*, 1st ed.; CRC Press: Boca Raton, FL, 2005. (c) Nakamura, S.; Pearton, S. Fasol, G., *The Blue Laser Diod. The Complete Story*; Springer: Heidelberg, 2000.

(3) (a) Montes, V. A.; Pohl, R.; Shinar, J.; Anzenbacher, P., Jr. *Chem.—Eur. J.* **2006**, *12*, 4523. (b) Shi, Y.-W.; Shi, M.-M.; Huang, J.-C.; Chen, H.-Z.; Wang, M.; Liu, X.-D.; Ma, Y.-G.; Yang, B. *Chem. Commun.* **2006**, 1941. (c) Pohl, R.; Montes, V. A.; Shinar, J.; Anzenbacher, P., Jr. *J. Org. Chem.* **2004**, *69*, 1723. (d) Pohl, R.; Anzenbacher, P., Jr. *Org. Lett.* **2003**, *5*, 2769.

(4) (a) VanSlyke, S. A.; Bryan, P. S.; Lovercchio, F. V. U. S. Patent 5 150 006, **1990**. (b) Burrow, P. E.; Shen, Z.; Bulvoic, V.; McCarty, D. M.; Forrest, S. R.; Cronin, J. A.; Thompson, M. E. *J. Appl. Phys.* **1996**, *79*, 7991. (c) Sugimoto, M.; Anzai, M.; Sakanoue, K.; Sakaki, S. *Appl. Phys. Lett.* **2001**, *79*, 2348. (d) Chen, C. H.; Shi, J. *Coord. Chem. Rev.* **1998**, *171*, 161.

(5) (a) Nagendran, S.; Roesky, H. W. *Organometallics* **2008**, *27*, 457. (b) Hopkins, T. A.; Meerholz, K.; Shaheen, S.; Anderson, M. L.; Schmidt, A.; Kippelen, B.; Padias, A. B.; Hall, H. K., Jr.; Peyghambarian, N.; Armstrong, N. R. *Chem. Mater.* **1996**, *8*, 344. (c) Kido, J.; Endo, J. *Chem. Lett.* **1997**, 593. (d) Kido, J.; Iizumi, Y. *Chem. Lett.* **1997**, 963. (e) Sapochak, L. S.; Padmaperuma, A.; Washton, N.; Endrino, F.; Schmetz, G. T.; Marshall, J.; Fogarty, D.; Burrows, P. E.; Forrest, S. R. *J. Am. Chem. Soc.* **2001**, *123*, 6300. (f) Yuchi, A.; Hiramatsu, H.; Ohara, M.; Ohata, N. *Anal. Sci.* **2003**, *19*, 1177. (g) Yu, J.; Chen, Z.; Sakuratani, Y.; Suzuki, H.; Tokita, M.; Miyata, S. *Jpn. J. Appl. Phys.* **1999**, *38*, 6762.

(6) (a) Deda, M. L.; Aiello, I.; Grisolia, A.; Ghedini, M.; Amati, M.; Lelj, F. *Dalton Trans.* **2006**, 330. (b) Bryan, P. S.; Lovercchio, F. V.; VanSlyke, S. A. U.S. Patent 5 141 671, **1992**. (c) Deaton, J. C.; Place, D. W.; Brown, C. T.; Rajeswaran, M.; Kondakova, M. E. *Inorg. Chim. Acta* **2008**, *361*, 1020. (d) So, S.; Lee, K.; Choi, W.; Leung, L.; Lo, W. *Jpn. J. Appl. Phys.* **2001**, *40*, 5959. (e) Shen, Z.; Burrows, P. E.; Bulovic, V.; Forrest, S. R.; Thompson, M. E. *Science* **1997**, *276*, 2009. (f) Qiu, Y.; Shao, Y.; Zhang, D.; Hong, X. *Jpn. J. Appl. Phys.* **2000**, *39*, 1151. (g) Giro, G.; Cocchi, M.; Di Marco, P.; Fattori, V.; Dembech, P.; Rizzoli, S. *Synth. Met.* **2001**, *123*, 529.

(7) (a) Shi, J.; Chen, C. H.; Klubek, K. P. U.S. Patent 75 897, **1997**. (b) Liu, S.-F.; Seward, C.; Aziz, H.; Hu, N.-X.; Popovic, Z.; Wang, S. *Organometallics* **2000**, *19*, 5709.

example of an investigation of photophysical properties and molecular orbital distribution in heteroleptic aluminum complexes with two six-membered chelating rings.

In this regard, 2-(2*H*-benzo[*d*][1,2,3]triazol-2-yl)-4,6-di-*tert*-pentylphenol (**Lig¹H**) and 2-*tert*-butyl-6-(5-chloro-2*H*-benzo[*d*][1,2,3]triazol-2-yl)-4-methylphenol (**Lig²H**) were employed as logical chelating ligands, because they are affordable starting materials used industrially as UV stabilizers and are likely to form heteroleptic aluminum complexes with two six-membered rings due to steric congestion of **Lig¹** or **Lig²** in the vicinity of the aluminum. Herein we report on the synthesis, characterization, X-ray structures, photoluminescent properties, and theoretical DFT studies of novel aluminum complexes **1–5** containing **Lig¹** or **Lig²**.

Experimental Section

General Considerations. All manipulations were carried out under a dinitrogen atmosphere using standard Schlenk and glovebox techniques.⁸ All other chemicals were purchased from Aldrich and were used as supplied unless otherwise indicated. Toluene, hexane, and tetrahydrofuran (THF) were dried with Na/K alloy with benzophenone and were stored over activated 3 Å molecular sieves.⁹ All deuterium solvents were dried over activated molecular sieves (3 Å) and were used after vacuum transfer to a Schlenk tube equipped with a J. Young valve.⁹

Measurements. ¹H and ¹³C{¹H} spectra were recorded at ambient temperature on a Bruker AVANCE 400 NMR spectrometer using standard parameters. The chemical shifts are referenced to the peaks of residual CDCl₃ (δ 7.24, ¹H NMR; δ 77.0, ¹³C{¹H} NMR). Elemental analyses and EI-mass data were performed by EA 1110-FISONS(CE) and JMS 700, respectively. UV–vis and PL spectra were recorded on a Jasco V-530 and a Spex Fluorog-3 Luminescence spectrophotometer, respectively. Thermogravimetric analyses (TGA) were carried out under a nitrogen atmosphere at a heating rate of 10 °C/min with a Dupont 9900 analyzer. UV–visible absorption and fluorescence measurements were performed in THF with a 1 cm quartz cuvette at ambient temperature. Quantum yields were determined using quinine sulfate (Fluka) as the standard (1×10^{-6} M in 0.5 M H₂SO₄, Φ_F = 0.55).¹⁰

Synthesis of Complexes 1–5. **Synthesis of 1.** To a stirred colorless solution of AlMe₃ (2.0 M solution in toluene, 1.0 mL, 2.0 mmol) in 30 mL of toluene was added dropwise at –78 °C a solution of **Lig¹H** (1.44 g, 4.0 mmol) in 20 mL of toluene. The reaction mixture was allowed to warm to room temperature and then refluxed for 1 h. The residue, obtained by removing the solvent under vacuum, was redissolved in 20 mL of toluene, and phenol (0.188 g, 2.0 mmol) in 10 mL of toluene was added and then refluxed for 1 h. All volatiles were removed under vacuum, and the residue was washed with 20 mL of *n*-hexane three times. The desired product **1** was isolated as yellow crystals after the methylene chloride/*n*-hexane solution remained at –20 °C in a refrigerator for a few days (1.40 g, 85%).

¹H NMR (CDCl₃, 400.15 MHz, ppm): δ 8.27 (s, 2H), 8.09 (d, 2H), 7.96 (d, 2H), 7.43 (m, 2H), 7.14 (s, 2H), 6.87 (t, 2H), 6.65 (d, 2H), 6.50 (t, 1H), 1.63 (q, 4H), 1.30 (s, 12H), 1.02 (s, 4H), 0.92 (s, 6H), 0.81 (s, 6H), 0.62 (q, 6H), 0.02 (q, 6H). ¹³C{¹H} NMR (CDCl₃, 100.63 MHz, ppm): δ 159.00, 148.92, 142.43, 140.36, 139.72, 138.40, 129.10, 128.96, 127.87, 127.52, 126.19, 119.17,

117.87, 117.26, 116.86, 38.62, 37.62, 37.53, 36.91, 31.52, 28.57, 28.39, 27.13, 26.98, 9.06, 8.76. ²⁷Al NMR (CDCl₃, 52.105 MHz, ppm): δ 82.93. EI-MS: calcd 821, found 821. Anal. Calcd for C₅₀H₆₁N₆O₃Al: C, 73.14; H, 7.49; N, 10.24. Found: C, 73.99; H, 7.78; N, 10.45.

Synthesis of 2. The desired product **2** was obtained as yellow solids in an isolated yield of 80% (1.43 g) in a manner analogous to the procedure for **1** using AlMe₃ (2.0 M solution in toluene, 1.0 mL, 2.0 mmol), **Lig¹H** (1.44 g, 4.0 mmol), and 4-phenylphenol (0.34 g, 2.0 mmol).

¹H NMR (CDCl₃, 400.15 MHz, ppm): δ 8.28 (d, 2H), 8.10 (br s, 2H), 7.96 (d, 2H), 7.43 (m, 4H), 7.37 (d, 2H), 7.28 (t, 2H), 7.14 (s, 4H), 6.71 (d, 2H), 1.63 (q, 4H), 1.30 (s, 12H), 1.02 (m, 4H), 0.95 (s, 6H), 0.82 (s, 6H), 0.66 (t, 6H), 0.05 (t, 6H). ¹³C{¹H} NMR (CDCl₃, 100.63 MHz, ppm): δ 158.82, 148.89, 142.46, 141.20, 140.38, 139.73, 138.46, 130.53, 129.08, 128.46, 127.90, 127.76, 127.58, 126.19, 125.87, 119.37, 117.93, 117.21, 116.87, 38.64, 37.64, 36.93, 31.53, 28.60, 28.40, 27.16, 27.00, 9.08, 8.80. ²⁷Al NMR (CDCl₃, 52.105 MHz, ppm): δ 89.21. EI-MS: calcd 897, found 897. Anal. Calcd for C₅₆H₆₅N₆O₃Al: C, 74.97; H, 7.30; N, 9.37. Found: C, 74.38; H, 7.44; N, 9.43.

Synthesis of 3. The desired product **3** was obtained as yellow solids in an isolated yield of 82% (1.20 g) in a manner analogous to the procedure for **1** using AlMe₃ (2.0 M solution in toluene, 1.0 mL, 2.0 mmol), **Lig²H** (1.26 g, 4.0 mmol), and phenol (0.34 g, 2.0 mmol).

¹H NMR (CDCl₃, 400.15 MHz, ppm): δ 8.11 (s, 3H), 8.05–7.83 (m, 3H), 7.42 (m, 2H), 7.06 (s, 2H), 6.92 (m, 1H), 6.67 (q, 2H), 6.56 (t, 1H), 2.29 (s, 6H), 0.80 (s, 18H). ¹³C{¹H} NMR (CDCl₃, 100.63 MHz, ppm): δ 149.13, 144.75, 142.31, 135.31, 133.72, 130.60, 130.12, 129.39, 127.21, 126.30, 119.36, 118.93, 118.36, 116.91, 116.69, 34.75, 31.57, 28.78, 22.63, 20.84, 14.08. ²⁷Al NMR (CDCl₃, 52.105 MHz, ppm): δ 80.80. EI-MS: calcd 749, found 748. Anal. Calcd for C₄₀H₃₉N₆O₃Cl₂Al: C, 64.09; H, 5.23; N, 11.21. Found: C, 63.84; H, 5.57; N, 11.85.

Synthesis of 4. The desired product **4** was obtained as yellow solids in an isolated yield of 87% (1.44 g) in a manner analogous to the procedure for **1** using AlMe₃ (2.0 M solution in toluene, 1.0 mL, 2.0 mmol), **Lig²H** (1.26 g, 4.0 mmol), and 4-phenylphenol (0.34 g, 2.0 mmol).

¹H NMR (CDCl₃, 400.15 MHz, ppm): δ 8.14 (s, 3H), 8.10–7.75 (m, 3H), 7.50–7.15 (m, 9H), 7.08 (s, 2H), 6.71 (m, 2H), 2.32 (s, 6H), 0.85 (s, 18H). ¹³C{¹H} NMR (CDCl₃, 100.63 MHz, ppm): δ 158.38, 149.16, 149.10, 142.96, 142.00, 140.95, 140.54, 135.39, 133.77, 131.14, 130.72, 130.20, 130.16, 129.46, 128.70, 128.51, 128.10, 128.05, 128.02, 127.29, 127.25, 126.27, 126.08, 119.40, 119.35, 119.17, 118.99, 118.38, 116.98, 116.65, 34.79, 28.80, 20.88. ²⁷Al NMR (CDCl₃, 52.105 MHz, ppm): δ 83.00. EI-MS: calcd 825, found 825. Anal. Calcd for C₄₆H₄₃N₆O₃Cl₂Al: C, 66.91; H, 5.25; N, 10.18. Found: C, 66.52; H, 5.44; N, 10.15.

Synthesis of 5. To a stirred yellow solution of complex **1** (0.787 g, 1.0 mmol) in 30 mL of toluene was added H₂O (18 μL, 1.0 mmol) at room temperature, and then the mixture was refluxed for 12 h. The residue, obtained by removing the solvent under vacuum, was recrystallized in *n*-hexane. The desired product **5** was isolated as pale yellow crystals after the solution remained at –20 °C in a refrigerator for a few days (0.59 g, 80%).

¹H NMR (CDCl₃, 400.15 MHz, ppm): δ 8.22 (d, 2H), 8.10 (br s, 1H), 7.74 (br s, 1H), 7.53 (m, 2H), 7.40 (d, 1H), 2.05 (q, 2H), 1.74 (q, 2H), 1.48 (s, 6H), 1.41 (s, 6H), 0.72 (m, 6H). ¹³C{¹H} NMR (CDCl₃, 100.63 MHz, ppm): δ 153.76, 147.04, 136.49, 131.58, 129.05, 128.23, 127.45, 118.76, 118.04, 39.49, 38.60, 36.95, 33.46, 28.42, 28.03, 9.56, 9.21. ²⁷Al NMR (CDCl₃, 52.105 MHz, ppm): δ 84.86. Anal. Calcd for C₈₈H₁₁₂N₁₂O₅Al₂: C, 71.81; H, 7.67; N, 11.42. Found: C, 72.29; H, 7.86; N, 11.75.

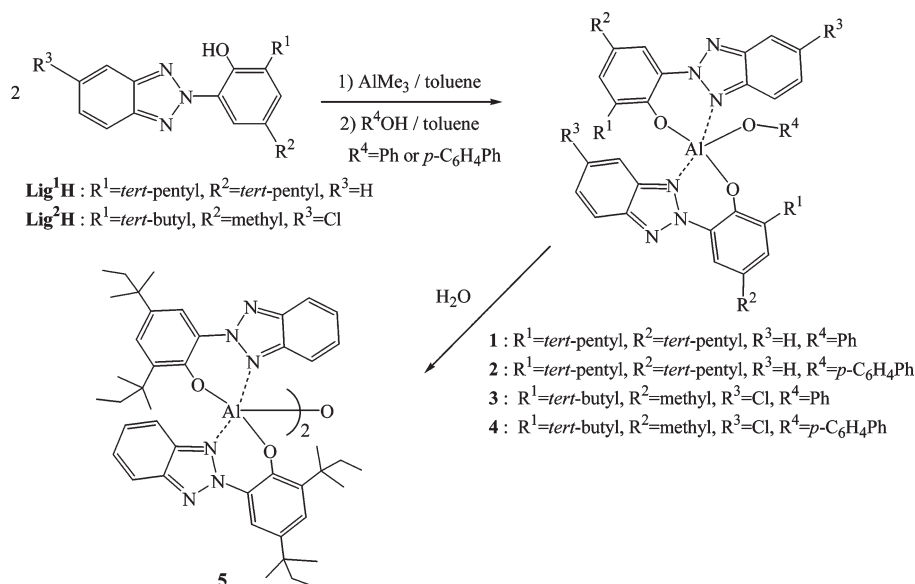
X-ray Structure Determination for 1, 3, and 5. Reflection data for **1**, **3**, and **5** were collected on a Bruker APEX II CCD area diffractometer with graphite-monochromated Mo Kα radiation

(8) (a) Shriver, D. F. In *The Manipulation of Air-Sensitive Compounds*; McGraw-Hill: New York, 1969. (b) Errington, R. J. In *Advanced Practical Inorganic and Metalorganic Chemistry*; Blackie Academic & Professional: London, 1997.

(9) Armarego, W. L. F.; Chai, C. L. L. In *Purification of Laboratory Chemicals*, 5th ed.; Elsevier: New York, 2003.

(10) (a) Melhuish, W. H. *J. Phys. Chem.* **1961**, 65, 229. (b) Demas, J. N.; Crosby, G. A. *J. Phys. Chem.* **1971**, 75, 991.

Scheme 1. Synthetic Routes to Complexes 1–5



($\lambda = 0.7107 \text{ \AA}$). Specimens of suitable quality and size were selected, mounted, and centered in the X-ray beam by using a videocamera. The hemisphere of reflection data was collected as ω -scan frames with $0.3^\circ/\text{frame}$ and an exposure time of 5 s/frame. Cell parameters were determined and refined by the SMART program.¹¹ Data reduction was performed using SAINT software.¹² The data were corrected for Lorentz and polarization effects. An empirical absorption correction was applied using the SADABS program.¹³ The structures of the compounds were solved by direct methods and refined by full matrix least-squares methods using the SHELXTL program package with anisotropic thermal parameters for all non-hydrogen atoms.¹⁴ X-ray crystal structures of **1**, **3**, and **5** were drawn by the Diamond Program ver. 2.1e.

Computational Details. The ground-state (S_0) structures and the first singlet excited-state (S_1) structures of complexes were optimized using the ab initio Hartree–Fock (HF) with the

6-31G(d) basis sets and using CIS¹⁵ with the 6-31G basis set, respectively. To obtain the electronic transition energies, which include some account of electron correlation, TD-DFT¹⁶ using the hybrid B3LYP¹⁷ (TD-B3LYP) functional was used with the 6-31G(d) basis set. Emission wavelengths were evaluated on the CIS-optimized structures of the excited state. For comparison with emission wavelengths, absorption wavelengths were predicted on the HF-optimized structures of the ground state (see Supporting Information). All calculations described here were carried out with the GAUSSIAN 03 program.¹⁸

Result and Discussion

Compounds **1–4** were obtained with high yield (> 80%) by adding dropwise a 2 equiv amount of **Lig¹H** or **Lig²H** in toluene to a solution of AlMe_3 and subsequent addition of ROH ($\text{R} = \text{Ph}$ or $p\text{-C}_6\text{H}_4\text{Ph}$), as outlined in Scheme 1. The compounds were purified by washing with *n*-hexane and recrystallized in methylene chloride. Complex **1** was also produced when 1 equiv of **Lig¹H** and excess AlMe_3 were mixed in toluene solution. Thus, the formation of **1** appears to be kinetically and thermodynamically favored in this reaction, whereas the compositions of other heteroleptic aluminum compounds are sensitive to the ratios of the starting materials.¹⁹

The hydrolysis of alkoxide has proven to be a useful route to the formation of various metallic and metalloidal oxo complexes.²⁰ Thus the addition of H_2O into the toluene solution of complexes **1** gave oxo-bridged aluminum dimeric complex **5** with 80% isolated yield, which was remarkably stable in a solid state for more than a month. In addition, according to ^1H NMR spectroscopy, **5** is very stable at room temperature for more than a week in chloroform- d_1 , acetone- d_6 , and methanol- d_4 solutions contained in capped NMR tubes. Compound **5** is soluble in a variety of solvents

(11) SMART Version 5.0, Data Collection Software; Bruker AXS Inc.: Madison, WI, 1998.

(12) SAINT Version 5.0, Data Integration Software; Bruker AXS Inc.: Madison, WI, 1998.

(13) Sheldrick, G. M. SADABS: Program for Absorption Correction with Bruker SMART System; University Göttingen: Germany, 1996.

(14) Sheldrick, G. M. SHELXS-97: Program for the Solution of Crystal Structures; University Göttingen: Germany, 1990.

(15) Foresman, J. B.; Head-Gordon, M.; Pople, J. A.; Frisch, M. J. *J. Phys. Chem.* **1992**, 96, 135.

(16) Runge, E.; Gross, E. K. *Phys. Rev. Lett.* **1984**, 52, 997.

(17) Stephens, P. J.; Devlin, F. J.; Chabalowski, C. F.; Frisch, M. J. *J. Phys. Chem.* **1994**, 98, 11623–11627.

(18) Frisch, M. J.; Trucks, G. W.; Schlegel, H. B.; Scuseria, G. E.; Robb, M. A.; Cheeseman, J. R.; Montgomery, J. A., Jr.; Vreven, T.; Kudin, K. N.; Burant, J. C.; Millam, J. M.; Iyengar, S. S.; Tomasi, J.; Barone, V.; Mennucci, B.; Cossi, M.; Scalmani, G.; Rega, N.; Petersson, G. A.; Nakatsuji, H.; Hada, M.; Ehara, M.; Toyota, K.; Fukuda, R.; Hasegawa, J.; Ishida, M.; Nakajima, T.; Honda, Y.; Kitao, O.; Nakai, H.; Klene, M.; Li, X.; Knox, J. E.; Hratchian, H. P.; Cross, J. B.; Bakken, V.; Adamo, C.; Jaramillo, J.; Gomperts, R.; Stratmann, R. E.; Yazyev, O.; Austin, A. J.; Cammi, R.; Pomelli, C.; Ochterski, J. W.; Ayala, P. Y.; Morokuma, K.; Voth, G. A.; Salvador, P.; Dannenberg, J. J.; Zakrzewski, V. G.; Dapprich, S.; Daniels, A. D.; Strain, M. C.; Farkas, O.; Malick, D. K.; Rabuck, A. D.; Raghavachari, K.; Foresman, J. B.; Ortiz, J. V.; Cui, Q.; Baboul, A. G.; Clifford, S.; Cioslowski, J.; Stefanov, B. B.; Liu, G.; Liashenko, A.; Piskorz, P.; Komaromi, I.; Martin, R. L.; Fox, D. J.; Keith, T.; M. A. Al-Laham, Peng, C. Y.; Nanayakkara, A.; Challacombe, M.; Gill, P. M. W.; Johnson, B.; Chen, W.; Wong, M. W.; Gonzalez, C.; Pople, J. A. *Gaussian 03*, Revision C.02; Gaussian, Inc.: Wallingford, CT, 2004.

(19) Lewinski, J.; Zachara, J.; Starowieyski, K. B.; Ochal, Z.; Justyniak, I.; Kopec, T.; Stolarzewicz, P.; Dranka, M. *Organometallics* **2003**, 22, 3773.

(20) (a) Kushi, Y.; Fernando, Q. *J. Am. Chem. Soc.* **1970**, 92, 91. (b) VanSlyke, S. A. U.S. Patent 5 151 629, **1992**. (c) Papadimitrakopoulou, F.; Zhang, X.-M.; Thomsen, D. L.; Higginson, K. A. *Chem. Mater.* **1996**, 8, 1363.

Table 1. Crystallographic Data and Parameters for **1**, **3**, and **5**

	1	3	5
empirical formula	C ₅₀ H ₆₁ AlN ₆ O ₃	C ₄₀ H ₃₈ AlCl ₂ N ₆ O ₃	C ₉₁ H ₁₂₂ Al ₂ Cl ₆ N ₁₂ O ₇
fw	821.03	748.64	1762.67
cryst syst	triclinic	monoclinic	orthorhombic
space group	$P\bar{1}$	$P2_1/c$	$Ccc2$
<i>a</i> (Å)	11.2879(4)	15.6237(17)	17.8534(14)
<i>b</i> (Å)	12.6897(5)	20.907(2)	21.9402(17)
<i>c</i> (Å)	17.3676(7)	15.0343(18)	24.7375(18)
α (deg)	102.212(2)	90	90
β (deg)	104.375(2)	114.863(7)	90
γ (deg)	93.132(2)	90	90
<i>V</i> (Å ³)	2340.18(16)	4455.8(9)	9689.9(13)
<i>Z</i>	2	4	4
<i>d</i> _{calcd} (g/cm ³)	1.165	1.116	1.208
<i>F</i> (000)	880	1564	3744
cryst size (mm)	0.20 × 0.15 × 0.10	0.15 × 0.14 × 0.11	0.40 × 0.12 × 0.11
<i>T</i> (K)	130	130	130
θ range (deg)	1.24 ≤ θ ≤ 31.82	1.44 ≤ θ ≤ 20.22	1.69 ≤ θ ≤ 25.75
no. of unique reflns	84 871	24 443	15 851
no. of obsd reflns (<i>I</i> > 2 σ (<i>I</i>))	15 122	4263	7724
no. of params refined	603	487	555
<i>R</i> ₁ (<i>I</i> > 2 σ (<i>I</i>)) ^a	0.0566	0.0844	0.0792
<i>wR</i> ₂ (<i>I</i> > 2 σ (<i>I</i>)) ^b	0.1865	0.1678	0.1893
GOF(<i>I</i> > 2 σ (<i>I</i>))	1.027	1.007	1.027

$$^a R_1 = \|F_o\| - \|F_c\|/\|F_o\|, ^b wR_2 = [w(F_o^2 - F_c^2)^2/w(F_o^2)^2]^{1/2}.$$

including toluene, methanol, acetone, and *n*-hexane. Although some examples of oxo-bridged aluminum complexes such as (Q₂Al)₂O have been reported,^{20a} their stabilities could not satisfy the requirement for application because of their unfilled coordination sites. However, compound **5** has extremely higher thermal stability than other pentacoordinated systems.

Compounds **1–5** have also been investigated with respect to thermal stability under a dinitrogen atmosphere using TGA. TGA measurements exhibit high DT₅ values (5.0 wt % decomposition temperatures) of 220, 210, 207, 215, and 380 °C for **1–5**, respectively. This data reflect that the Lig¹–Al or Lig²–Al bond is thermally robust. Most interestingly, complex **5** has extremely high thermal stability probably originated from the strong Al–O–Al bond. All complexes **1–5** are air-stable in both the solid and solution states, probably due to the steric protection of the Al center by two *tert*-pentyl or *tert*-butyl groups at the R¹ position as well as the three strong Al–O bonds.

Compounds **1–5** were characterized by ¹H, ¹³C{¹H}, and ²⁷Al NMR spectroscopy, EI-mass spectrometry, and elemental analysis. The structures of **1**, **3**, and **5** were determined by single-crystal X-ray crystallography. The electron-impact mass spectrum (70 eV) indicates monomeric behavior for **1–4** in the gas phase; however, the nonvolatile property of **5** is observed in the mass spectrum. The ¹H NMR spectra of **1–5** display well-defined sharp resonances with the expected integrations. Also, well-defined resonances for the aromatic and aliphatic carbons are observed in the ¹³C{¹H} NMR spectrum, and there is no indication of the presence of higher oligomers because the resonances consist of very sharp and intense singlets. Despite a high quadrupolar relaxation rate for the ²⁷Al nucleus (*I* = 5/2), a single broad ²⁷Al NMR chemical shift at 82.93, 89.21, 80.80, 83.00, and 84.86 ppm for **1–5**, respectively, was detected at room

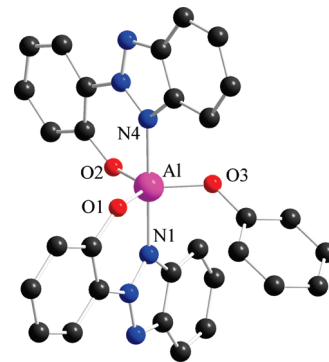


Figure 1. X-ray structures of compounds **1** and its atom labeling (H atoms and *tert*-pentyl groups were omitted for clarity). Selected bond lengths (Å) and angles (deg): Al–O1 1.7509(13), Al–O2 1.7504(12), Al–O3 1.7531(13), Al–N1 2.0151(15), Al–N2 2.0134(15), O1–Al–O2 117.18(6), O1–Al–O3 120.99(6), O2–Al–O3 121.81(6), O1–Al–N1 89.60(6), O2–Al–N1 90.08(6), O3–Al–N1 91.87(6), O1–Al–N4 90.70(6), O2–Al–N4 89.04(6), O3–Al–N4 88.69(6), N1–Al–N4 179.11(6).

temperature in chloroform-*d*₁. These peaks can be reasonably assigned to a pentacoordinated aluminum atom, which is normally observed in the range 60–100 ppm.²¹ These results are consistent with X-ray structures of **1**, **3**, and **5** in the solution phase.

To elucidate the nature of the metal–ligand bonding and the solid-state structural nature of **1**, **3**, and **5**, we carried out a single-crystal X-ray diffraction study. Single crystals suitable for X-ray structural determination were obtained by cooling of a solution of either methylene chloride/*n*-hexane for **1** and **3** or *n*-hexane for **5** at –20 °C. The X-ray structures, selected bond distances, and selected bond angles for **1**, **3**, and **5** are shown in Figures 1–3, respectively. The complexes **1**, **3**, and **5** crystallized in space group $P\bar{1}$, $P2_1/c$, and $P22a$, respectively. In order to examine the distortion of the coordination geometry in **1**, **3**, and **5**, the parameters τ ($\tau = (\beta - \alpha)/60$, where α and β are the largest and next-largest

(21) (a) Potapov, A. G.; Terskikh, V. V.; Zakharov, V. A.; Bukatov, G. D. *J. Mol. Catal. A: Chem.* **1999**, *145*, 147. (b) Potapov, A. G.; Terskikh, V. V.; Bukatov, G. D.; Zakharov, V. A. *J. Mol. Catal. A: Chem.* **1997**, *122*, 61.

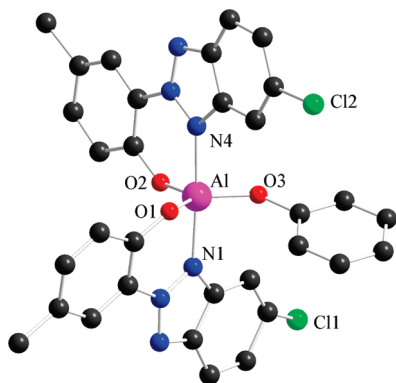


Figure 2. X-ray structures of compounds **3** and its atom labeling (H atoms and two *tert*-butyl groups were omitted for clarity). Selected bond lengths (Å) and angles (deg): Al–O1 1.742(7), Al–O2 1.737(7), Al–O3 1.721(7), Al–N1 2.022(9), Al–N4 2.008(8), O1–Al–O2 118.6(3), O1–Al–O3 123.7(4), O2–Al–O3 117.7(4), O1–Al–N1 87.7(4), O2–Al–N1 89.8(3), O3–Al–N1 92.8(4), O1–Al–N4 91.7(3), O2–Al–N4 87.5(3), O3–Al–N4 90.3(3), N1–Al–N4 176.5(4).

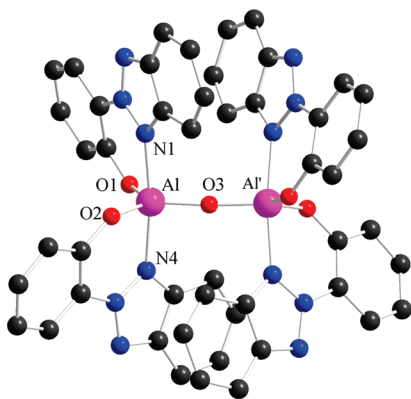


Figure 3. X-ray structures of compounds **5** and its atom labeling (H atoms and *tert*-pentyl groups were omitted for clarity). Selected bond lengths (Å) and angles (deg): Al–O1 1.762(4), Al–O2 1.760(4), Al–O3 1.6900(17), Al–N1 2.051(6), Al–N4 2.050(6), O1–Al–O2 120.5(2), O1–Al–O3 119.00(17), O2–Al–O3 120.47(16), O1–Al–N1 88.0(2), O2–Al–N1 87.8(2), O3–Al–N1 94.2(3), O1–Al–N4 89.0(2), O2–Al–N4 87.6(2), O3–Al–N4 93.5(3), N1–Al–N4 172.3(2), Al–O3–Al' 176.3(5).

interligand bond angle, respectively)²² and Δ (dihedral angle method)²³ were calculated. For the regular trigonal-bipyramidal complexes, the trigonality parameter τ will be 1.0, and it decreases to zero as the square-pyramidal distortion increases. Similarly, Δ is zero for trigonal-bipyramidal compounds and 1.0 for square-pyramidal complexes. The calculated τ and Δ values are 0.96 and 0.06 for **1**, 0.88 and 0.07 for **3**, and 0.86 and 0.21 for **5**, respectively, indicating nearly ideal trigonal-bipyramidal geometry. Figures 1–3 show that the above calculations fit well for complexes **1**, **3**, and **5**. Thus, in addition to the three “anionic” oxygens, the aluminum atom is ligated by means of two nitrogen atoms stem-

ming from the benzotriazole ligands, lending slightly distorted trigonal-bipyramidal geometry around the aluminum. The equatorial oxygens form a regular triangle with sides of 3.033(2) Å for **1**, 3.003(4) Å for **3**, and 3.009(2) Å for **5**. The average distances between these oxygens and the axial nitrogens are 2.669(2) for **1**, 2.657(7) Å for **3**, and 2.686(2) Å for **5**. The sum of the O_{eq} –Al– O_{eq} angles is 359.98(6)° for **1**, 360.0(4)° for **3**, and 359.97(20)° for **5** [average O_{eq} –Al– O_{eq} angle is 119.99(6)° for **1**, 120.0(4)° for **3**, and 119.99(19)° for **5**], and the N_{axial} –Al– N_{axial} angles (179.11(16)° for **1**, 176.5(4)° for **3**, and 172.3(2)° for **5**) are nearly linear. The average Al–O [1.751(2) Å for **1**, 1.733(3) Å for **3**, and 1.737(4) Å for **5**] and Al–N [2.0142(15) Å for **1**, 2.015(9) Å for **3**, and 2.050(6) Å for **5**] bond distances are similar to the average distances observed for other structurally characterized aluminum alkoxides or aluminum amides, respectively.^{6a,24}

To examine the optical properties of **1**–**5**, UV–vis and PL experiments were carried out, and the absorption (left) and emission (right) spectra of **1**–**5** in chloroform are shown in Figure 4. All complexes **1**–**5** feature major absorption bands at around 374–386 nm assigned to ligand-centered π – π^* transitions. As the ancillary ligand is varied from OPh to OC_6H_4 -*p*-Ph (from **1** to **2** or from **3** to **4**), the absorption maxima wavelength (λ_{abs}) is slightly blue-shifted. ϵ values of complexes **1**–**5** are in the range $(1.7$ – $4.5) \times 10^4$ M^{−1} cm^{−1}, which are considerably higher than for other Al systems.^{2a,24} Particularly, complex **5** gives a 2-fold higher ϵ value than other complexes **1**–**4** due to its dinuclear structure.

The PL emission spectra of **1**–**5** exhibit emission maxima (λ_{em}) ranging from 475 to 497 nm (Figure 4). Unlike the UV–vis absorption spectra, the alteration of a phenoxy-type ancillary ligand did not cause a blue-shift of λ_{em} . Interestingly, **1**, **2**, and **5**, containing a **Lig**¹ ligand, emit a sky-blue light around 480 nm, which is 20 nm blue-shifted compared with 495 nm of Al(Meq)₂OPh.^{2a} The pyridylphenol ligand, a widely used ligand in the synthesis of aluminum complexes having six-membered chelating rings, has 3.84 eV of π – π^* transition energy,²⁵ which is blue-shifted compared with that (4.0 eV)²⁶ of 8-hydroxyquinoline due to a weak conjugation, supporting our experiments. Furthermore, the emission maxima for **3** and **4**, with a **Lig**² ligand, are observed around 495 nm and are 20 nm red-shifted compared with complexes **1** and **2**. The negligible effect of phenolato groups on the absorption and emission spectra may be attributed to their low contribution in the HOMO and LUMO.^{6a,24} Complexes **1**–**5** showed sufficient quantum efficiencies of 0.11–0.17 for OLED application. Also, they have very strong emissions and broad emission areas with a half-width of 150 nm in the emission spectra. These are probably influenced by the rigidity of coordinated ligand **Lig**¹ or **Lig**², which shows very strong absorption bands itself, caused by its steric bulkiness and π -conjugation.

To investigate the electronic transition and the electronic structures for complex **1**, time-dependent density functional theory (TD-DFT) calculations were carried out at the B3LYP/6-31G(d) approximation level, which has been used in previous literature.^{6a} The geometry of **1** for the calculation

(22) (a) Atwood, D. A.; Harvey, M. J. *Chem. Rev.* **2001**, *101*, 37. (b) Addison, A. W.; Rao, T. N.; Reedijk, J.; van Rijn, J.; Verschoor, G. C. *J. Chem. Soc., Dalton Trans.* **1984**, 1349.

(23) Meuterties, E. L.; Guggenberger, L. J. *J. Am. Soc. Chem.* **1974**, *96*, 1748.

(24) Hwang, K. Y.; Lee, M. H.; Jang, H.; Sung, Y.; Lee, J. S.; Kim, S. H.; Do, Y. *Dalton Trans.* **2008**, 1818.

(25) Kaczmarek, L.; Balicki, R. *J. Chem. Soc., Perkin Trans.* **1994**, 1603.

(26) (a) Halls, M. D.; Schlegel, H. B. *Chem. Mater.* **2001**, *13*, 2632.

(b) Perkampus, H. H.; Kortum, K. *Z. Anal. Chem.* **1962**, *190*, 111.

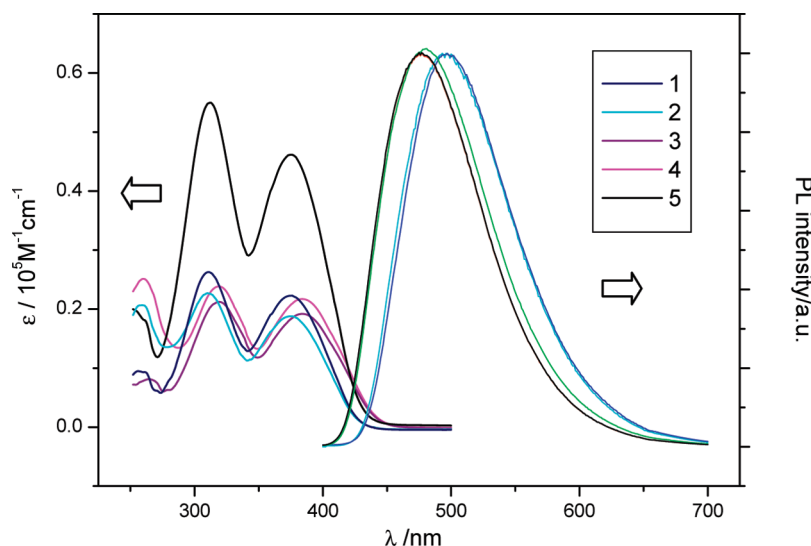


Figure 4. UV-vis absorption spectra (left) and PL emission spectra (right) of **1–5** in chloroform.

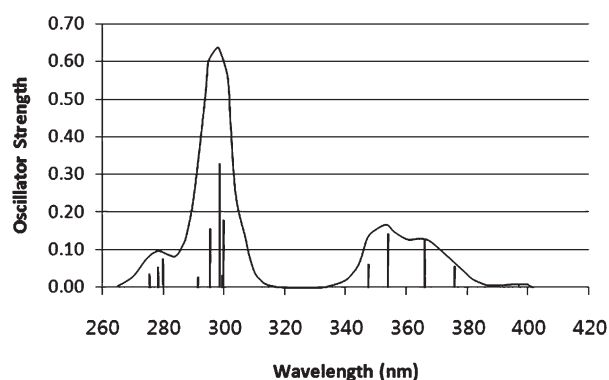


Figure 5. Simulated TD-DFT/B3LYP UV-vis absorption spectrum of complex **1** as a function of the 6-31G basis set employed in both the geometry optimization and the excitation energy determination.

Table 2. Computed Absorption Wavelengths (λ in nm) and Oscillator Strengths (f_{calc}) at the TD-B3LYP/6-31G(d) Level of Theory Using the HF/6-31G(d) Geometry for Complex **1**

state	λ (nm)	f_{calc}	nature	contribution
1	411.79	0.0026	HOMO \rightarrow LUMO	94%
2	396.71	0.0088	HOMO \rightarrow LUMO ₊₁	94%
3	375.82	0.0499	HOMO ₋₁ \rightarrow LUMO	93%
4	365.66	0.1180	HOMO ₋₁ \rightarrow LUMO ₊₁	93%
5	353.67	0.1359	HOMO ₋₂ \rightarrow LUMO	93%
6	347.32	0.0544	HOMO ₋₂ \rightarrow LUMO ₊₁	94%
7	309.68	0.0032	HOMO ₋₃ \rightarrow LUMO	91%
8	299.64	0.1704	HOMO ₋₄ \rightarrow LUMO	67%
9	299.44	0.0240	HOMO ₋₃ \rightarrow LUMO ₊₁	81%
10	298.34	0.3203	HOMO ₋₅ \rightarrow LUMO	76%
11	295.23	0.1474	HOMO ₋₄ \rightarrow LUMO ₊₁	78%
			HOMO ₋₄ \rightarrow LUMO	16%

was optimized from its X-ray structure. The computed optical data are listed in Table 2, and the simulated TD-DFT/B3LYP UV-vis absorption spectrum of complex **1** is shown in Figure 5, which matches roughly with actual UV-vis spectra of **1** in Figure 4. The optimized geometry and molecular orbitals for the first excited state of **1** are shown in Figure 6. Among the calculated absorptions and emissions, the absorption peak at 353.67 nm and the emission peak at 453.37 nm, the transition mainly from HOMO₋₂

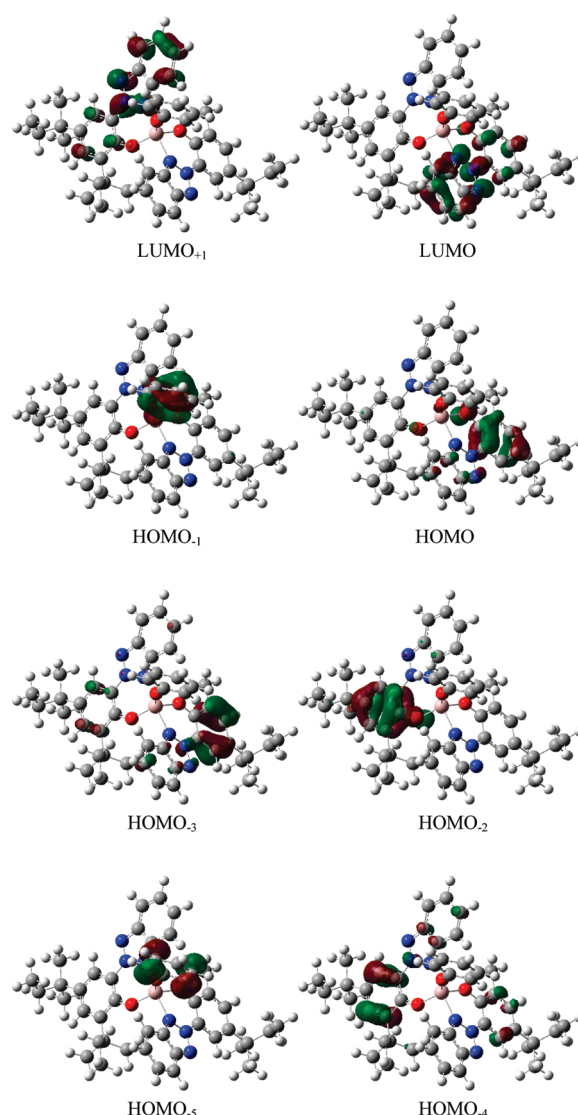


Figure 6. Frontier molecular orbitals for the first excited state of complex **1** from the B3LYP/CIS calculation.

to LUMO and from LUMO to HOMO, respectively, are considered to be dominant according to Tables 2 and 4 and

Table 3. Absorption Wavelengths (λ_{max} in nm) Computed at the TD-B3LYP Method Using the HF/6-31G(d)-Optimized Structures and the Emission Wavelengths (λ_{max} in nm) Computed at the TD-B3LYP Method Using the CIS/6-31G-Optimized Structures^a

compound	experiment		calculation	
	UV/vis	PL	TD-B3LYP//HF	TD-B3LYP//CIS
1	320, 376	475	295.23 (0.1474), 298.34 (0.3203) 353.67 (0.1359), 365.66 (0.1180)	453.37 (0.1512)

^aOscillator strengths are in parentheses.

Table 4. Computed Emission Wavelengths (λ in nm) and Oscillator Strengths (f_{calc}) at the TD-B3LYP/6-31G(d) Level of Theory Using the CIS/6-31G Geometry for Complex 1

state	λ (nm)	f_{calc}	nature	contribution
1	476.53	0.0085	HOMO ₋₁ → LUMO	73%
			HOMO → LUMO	25%
2	453.37	0.1512	HOMO → LUMO	50%
			HOMO ₋₁ → LUMO	21%
			HOMO ₋₂ → LUMO	14%
3	422.59	0.0954	HOMO ₋₂ → LUMO	82%
4	404.37	0.0403	HOMO → LUMO ₊₁	94%
5	394.37	0.0059	HOMO ₋₁ → LUMO ₊₁	97%

Figure 5, which is in good agreement with the experimental data of **1** in solution. As expected, there is little orbital contribution from the ancillary phenoxy group and Al metal center. This observation is well matched with the result that complex **5** showed a similar pattern in absorption and emission.

Because the HOMO and LUMO orbitals are likely localized on the phenoxy group and benzotriazole group of ligand **Lig**¹, respectively, this calculation supported our hypothesis that 10 and 20 nm red-shifted wavelengths of absorption and emission in complexes **3** and **4**, respectively, may result from attachment of chloride atom, an electron-withdrawing substituent, in the LUMO. If electron-donating

units are attached, a blue-shifted emitting material will be obtained. A trend of similar red- or blue-shift was observed in various homoleptic aluminum complexes containing substituents with high electron-donating or electron-withdrawing abilities at the 5,7-positions of the 8-hydroxyquinolate ligand, respectively.^{2a,3}

Conclusion

Novel aluminum complexes **1–5** having **Lig**¹ or **Lig**² ligands have been synthesized as blue-emitting materials and characterized by X-ray crystallography for **1**, **3**, and **5**. On the basis of their photophysical properties, they are strong candidates for blue-emitting materials for OLED application. Using DFT study, a strategy for fine-tuning the emission was established. Detailed studies on their tuning ability are in progress.

Acknowledgment. We gratefully acknowledge the Korea Research Foundation (KRF-2008-313-C00450).

Supporting Information Available: Frontier molecular orbitals for the ground state of complex **1** from the B3LYP//HF calculation and cif file for complexes **1**, **3**, and **5** are available free of charge via the Internet at <http://pubs.acs.org>.